Multi-messenger Astrophysics at Ultra-High Energy with the Pierre Auger Observatory

Jaime Alvarez-Muñiz[1] for the Pierre Auger Collaboration[2,*,**]

[1]Departamento de Física de Partículas & Instituto Galego de Física de Altas Enerxías, Universidade de Santiago de Compostela, 15782 Santiago de Compostela, Spain.
[2]Observatorio Pierre Auger, Av. San Martín Norte 304, 5613, Malargüe, Argentina.

Abstract. The study of correlations between observations of fundamentally different nature from extreme cosmic sources promises extraordinary physical insights into the Universe. With the Pierre Auger Observatory, we can significantly contribute to multi-messenger astrophysics by searching for ultra-high energy particles, particularly neutrinos and photons which, being electrically neutral, point back to their origin. Using Pierre Auger Observatory data, stringent limits at EeV energies have been established on the photon and neutrino fluxes from a large fraction of the sky, probing the production mechanisms of ultra-high energy cosmic rays. The good angular resolution and the neutrino identification capabilities of the Observatory at EeV energies allow the follow-up of events detected in gravitational waves, such as the binary mergers observed with the Advanced LIGO/Virgo detectors, or from other energetic sources of particles.

1 Introduction

Multi-messenger astronomy consists on the simultaneous observation of different messengers of the Universe namely, electromagnetic radiation, gravitational waves, neutrinos, and cosmic rays. These are in general created by different astrophysical processes and thus reveal different information about their sources.

The Pierre Auger Observatory [1] is a key detector in the field of multi-messenger astrophysics (see [2] for a recent review). Besides being primarily an Ultra-High Energy Cosmic Ray (UHECR) detector at energies above and around 10^{18} eV = 1 EeV with which several studies on properties of UHECR are being performed [3–7], the Auger detectors can also be used to efficiently identify two other messengers at ultra-high energy (UHE) namely photons and neutrinos [8–11].

UHE neutrinos are expected to be produced in the decay of charged pions created in interactions of UHECR in the sources and/or in their propagation through the cosmological radiation backgrounds (see for instance [12, 13] and refs. therein). Having no charge, neutrinos are not deflected in Galactic or inter-galactic magnetic fields and point back to the sites where they were produced. Being weakly-interacting particles, they can escape the cores of dense astrophysical objects and travel along cosmological distances practically without attenuation. At tens of EeV, neutrinos may be the only direct probe of the potential sources of UHECR at distances farther than $\sim$ 100 Mpc, revealing properties of the sources such as the evolution of their number density with redshift z [14]. UHE neutrinos can also aid in the localization of gravitational-wave (GW) sources recently observed with the LIGO and Virgo detectors [16–19] and enable a complementary study of their astrophysical progenitors. UHE photons are also produced in the decay of neutral pions created through the same mechanisms that generate the parent charged pions of the UHE neutrinos. However, and as opposed to neutrinos, photons undergo interactions with the extragalactic background light inducing electromagnetic cascades and this limits the volume from which EeV photons may be detected to distances of less than $\sim$ 5 Mpc at EeV energies [15].

In this work we describe the capabilities and performance of the Pierre Auger Observatory and report on searches for UHE neutrinos and photons in Auger. The null result allows us to put stringent upper bounds to the diffuse flux of neutrinos and photons as well as to the fluxes from point-like sources. These bounds significantly constrain many models of UHECR production. We also report on the follow-up in UHE neutrinos of GW events detected with the Advanced LIGO and Virgo detectors. Very recently, the IceCube detector observed a correlation an energetic neutrino candidate event and a gamma-ray flare from the powerful blazar TXS-0506+056 [20], along with a burst of events earlier in the same direction [21], hinting at the first identified source of neutrinos in the hundreds of TeV range. In this contribution we also report on the search for neutrinos from the blazar TXS 506+056 in the EeV range with Auger.

*e-mail: auger_spokepersons@fnal.gov
**Authors list: http://www.auger.org/archive/authors_2018_10.html

2 Neutrinos in Auger

The Pierre Auger Observatory is located in the Mendoza Province in Argentina at an average latitude $\lambda = 35.2^\circ$ South and at a mean atmospheric depth (altitude) of 880 g cm^{-2} ($\sim$ 1400 m above sea level) [1]. It has been running and taking data since its construction started in 2004. Auger consists of a surface detector (SD) of 1660 water-Cherenkov stations (WCD) spread over an area of 3000 km^2 in a triangular grid of 1.5 km spacing [1]. These are used to sample the particle front of air showers. The signals produced by the passage of shower particles through the SD stations are recorded as time traces in 25 ns intervals. The volume of atmosphere above the SD is monitored in clear and moonless nights with a Fluorescence Detector (FD) to observe the fluorescence emission of Nitrogen as the shower passes through the atmosphere [22].

Although the SD of the Pierre Auger Observatory is primarily an UHECR detector, air showers induced by UHE neutrinos can also be efficiently identified above 10^{17} eV in the background of UHECR [11]. The identification is based on a simple idea. UHECR arriving at Earth at highly inclined directions with respect to the vertical to the ground, interact shortly after entering the atmosphere and start extensive air showers whose electromagnetic component gets absorbed due to the large matter depth of atmosphere from the first interaction point to the ground. As a consequence, the shower front at ground level is dominated by muons and these induce sharp time traces in the WCD stations. On the contrary, showers induced by neutrinos at large zenith angles can start deep in the atmosphere, and a considerable fraction of electrons and photons reaches ground level. These undergo more interactions than muons in the atmosphere, spreading more in time as they pass through the detector. This is also the case for Earth-skimming (ES) showers, mainly induced by tau neutrinos (ν_τ) that traverse horizontally below the Earth's crust, and can interact near the surface inducing a tau lepton that escapes the Earth and decays in flight in the atmosphere above the SD [23]. With this simple idea in mind, firstly inclined showers are selected among the sample of events triggering the SD array. To discriminate neutrinos from UHECR, observables have been chosen related to the width of the signal trace and in particular the Area-over-Peak (AoP) of the digitized signal defined as the ratio of the integrated signal and its peak value.

Deeply-starting downward-going (DG) showers initiated by neutrinos of any flavor can be efficiently identified for zenith angles $60^\circ < \theta < 90^\circ$. A multivariate analysis (Fisher method) trained with Monte Carlo simulations of UHE neutrinos and a fraction ($< 20\%$) of real data is constructed combining several observables that carry information about the time spread of the signals in the WCD stations. An optimized cut on the Fisher variable is placed at a value that would yield one UHECR background event in 50 years. For optimization purposes of DG neutrinos, the total event sample has been divided in subsamples according to the reconstructed zenith angle with Downward-going high-angle (DGH) events $75^\circ < \theta < 90^\circ$ and Downward-going low-angle (DGL) events $58.5^\circ < \theta < 61.5^\circ$. These subsamples are further subdivided depending on the number of triggered stations for the DGH set, and the zenith angle for the DGL one with a different Fisher discrimination variable and optimized value of the cut in each subset.

In the ES channel, only ν_τ-induced showers with $90^\circ < \theta < 95^\circ$ can be efficiently detected. In this case the discrimination variable is directly the mean AoP ($\langle$AoP$\rangle$) of all the WCD stations triggered in the event. This channel is the most sensitive to UHE neutrinos, mainly due to the larger grammage and higher density of the Earth compared to the atmosphere where neutrinos are converted, and tau leptons can travel tens of kilometers at EeV energies. Full details of the inclined shower and neutrino selection criteria in Auger can be found in [11].

Applying these criteria a search for ES as well as DG neutrino-induced showers was performed in the Observatory data since 1 January 2004 when data taking started up to 30 June 2018. This corresponds to $\sim$ 9.5 equivalent years of operation of a complete SD or $\sim$ 14.5 years of lifetime because the array was not fully deployed until 2008. No neutrino candidates were identified in any of the selections ES, DGH or DGL. As an example in Fig. 1 we show the distribution of $\langle$AoP$\rangle$ in the whole data period compared to that expected in Monte Carlo simulations of neutrino-induced showers, along with the optimized value of the cut $\langle$AoP$\rangle$=1.83 above which an event would be regarded as a neutrino candidate in the ES channel. Remarkably $\sim$ 95% of the simulated neutrinos pass the inclined and neutrino identification criteria. This proves that Auger is a highly sensitive neutrino detector with its sensitivity limited mainly by its lifetime but not by the background due to UHECR-induced showers since this can be very efficiently reduced as shown in Fig. 1.

The non-observation of neutrino candidates in Auger data can be translated into an upper limit to the flux of UHE neutrinos. For this purpose the exposure of the SD of Auger needs to be calculated for the period of data taking. This is done with Monte Carlo simulations of neutrino-induced showers to which the same selection criteria as in data were also applied and the identification efficiencies of each channel - defined as the fraction of simulated events passing the cuts - were obtained [24]. In the case of Earth-skimming ν_τ induced showers, the efficiency depends on the energy of the emerging τ leptons E_τ, on the zenith angle θ and on the altitude h_c of the decay point of the τ above ground [25]. For downward-going neutrinos the identification efficiency depends on neutrino flavor, type of interaction (charged-current CC or neutral-current NC), neutrino energy E_ν, zenith angle θ, and distance D measured from the ground along the shower axis at which the neutrino is forced to interact in the simulations[11, 24]. In both cases, the identification efficiencies depend also on time because the SD array has been growing steadily from 2004 up to 2008 when it was completed, and because the fraction of working stations - although typically above 95% - is changing continuously with time.

For downward-going neutrinos the calculation of the exposure involves folding the identification efficiencies

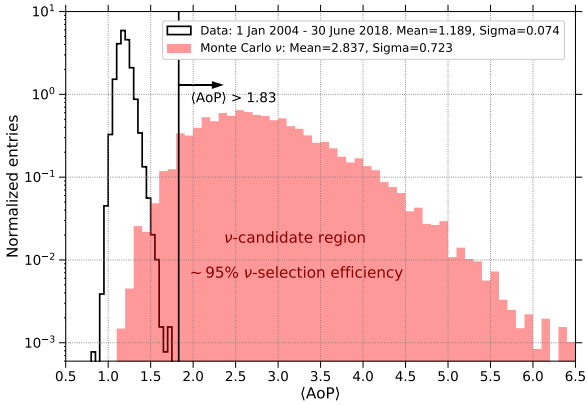

Figure 1. Distribution of ⟨AoP⟩ for the real events (black histogram) and Monte Carlo-simulated ν_τ events (red-shaded histogram) triggering the SD of Auger and that also fulfill the inclined Earth-Skimming (ES) selection criteria. Real data up to 30 June 2018. The vertical dashed line indicates the position of the optimized cut ⟨AoP⟩=1.83 above which an event would be regarded as a neutrino candidate. As indicated in the plot, ~ 95% of the simulated neutrinos pass the inclined and neutrino identification criteria.

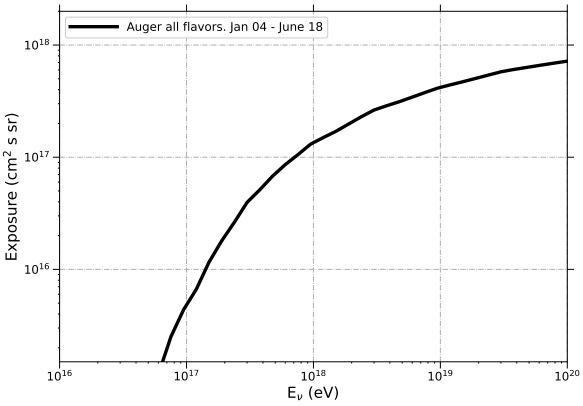

Figure 2. Exposure of the SD of the Pierre Auger Observatory (1 Jan. 2004 - 30 June 2018) as a function of neutrino energy E_ν obtained as the sum of the exposures for each neutrino flavor assuming a flavor mixture of $\nu_e : \nu_\mu : \nu_\tau = 1 : 1 : 1$

with the area of the SD projected onto the direction θ and with the ν interaction probability at a depth D for a neutrino energy E_ν depending on the CC or NC channel considered. Integrating over the parameter space (θ, D), in time over the search period, and summing over all the neutrino interaction channels yields the total exposure in the DG channel [11, 24]. In the Earth-skimming channel the identification efficiencies are also folded with the projected area of the SD, with the probability of a tau emerging from the Earth with energy E_τ (given a neutrino with energy E_ν crossing an amount of Earth determined by the zenith angle θ), as well as with the probability that the τ decays at an altitude h_c [25]. An integration over the whole parameter space (E_τ, θ, h_c) and time gives the exposure [11, 25].

The total exposure obtained as the sum of the individual exposures for each neutrino flavor assuming a flavor mixture of $\nu_e : \nu_\mu : \nu_\tau = 1 : 1 : 1$ is plotted in Fig. 2. The exposure is dominated by tauonic neutrinos because of the enhanced sensitivity in the Earth-skimming channel as explained before. The exposure folded with a differential energy flux of single-flavored UHE neutrinos and integrated in energy gives the expected number of events for that flux.

Assuming a differential neutrino flux $dN(E_\nu)/dE_\nu = k \cdot E_\nu^{-2}$, an upper limit on the value of k is obtained as $k_{90} = 2.39/\int_{E_\nu} E_\nu^{-2}\, \mathcal{E}_{\rm tot}(E_\nu)\, dE_\nu$, where 2.39 is the Feldman-Cousins factor [26] for non-observation of events in the absence of expected background accounting for systematic uncertainties [11]. The single-flavor 90% C.L. integrated limit we obtained in this work is $k_{90} < 4.4 \times 10^{-9}$ GeV cm^{-2} s^{-1} sr^{-1}. It applies in the energy interval $\sim 1.0 \times 10^{17}$ eV $- 2.5 \times 10^{19}$ eV for which ~ 90% of the total event rate for a E_ν^{-2} differential flux is expected. The integrated limit simply represents the value of the normalization of a E_ν^{-2} differential neutrino flux needed to produce 2.4 events. The denominator of the equation giving k_{90} can also be integrated in bins of energy, and a limit on k_{90} can also be obtained in each energy bin. This is displayed in Fig. 3. The differential limit is an effective way of characterizing the energy dependence of the sensitivity of a neutrino experiment. For the case of Auger it can be seen in Fig. 3 that the best sensitivity is achieved for energies around 1 EeV.

With this search we are strongly constraining models of cosmogenic neutrino production that assume pure protons at the sources with strong (FRII-type) evolution with redshift. For example, for the neutrino flux [31] corresponding to the upper edge of the red shaded area in Fig. 3, we expect ~ 6 events in Auger while none is detected, excluding that model at more than 90% CL. We are also starting to constrain models with moderate (Star-Formation-Rate, SFR) source evolution. For example for the model in [30] (shown as a dashed line in Fig. 3) that assumes pure proton and SFR-type evolution we expect ~ 2.3 events in Auger excluding this model at close to 90% C.L. At least a ~ 3-fold increase in the current Auger exposure will be needed to constrain at 90% C.L. the upper edge of the gray band in Fig. 3, a model that assumes a mixed composition for the primary UHECR [29]. Finally to be able to rule out at 90% C.L. the most optimistic predictions of cosmogenic neutrino flux at $10^{18} - 10^{19}$ eV if the primaries were pure iron [31], at least a 6-fold increase in exposure would be required, although this possibility is currently disfavored by recent results on the composition of UHECR [5, 48]. This is out of the range of the current configuration of Auger.

With the SD of the Pierre Auger Observatory we can also search for point-like sources of UHE neutrinos. This is possible due to the good angular resolution of Auger in the inclined directions, ~ 2.5°...0.5° improving typically with energy and zenith angle up to < 0.5° at $\theta > 60°$ and $E_\nu > 3$ EeV [33]. Given the little background ex-

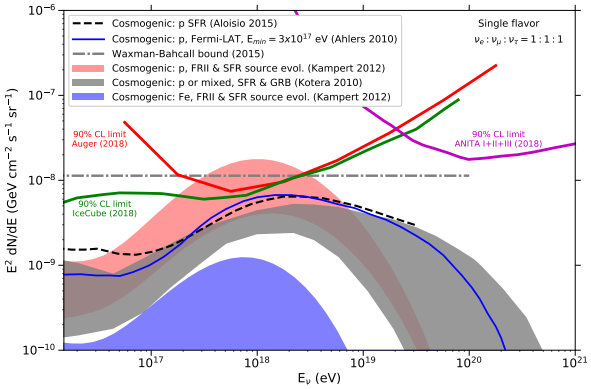

Figure 3. Pierre Auger Observatory differential upper limit (red curve) obtained with data up to 30 June 2018. We also show the most recent limits from ANITA [34] and IceCube [27] experiments, along with expected fluxes for several cosmogenic neutrino models [28–31] as well as the Waxman-Bahcall bound [32]. All differential limits in this plot are given for single flavor and converted to one energy decade. Neutrino flux models are also converted to single flavor when needed. A $\nu_e : \nu_\mu : \nu_\tau = 1 : 1 : 1$ flavor ratio at Earth is assumed.

pected with the optimized cuts on the neutrino discrimination variables any detection would be highly significant.

When addressing the sensitivity of the SD of Auger to point-like sources in the sky, it is important to keep in mind that the current analysis restricts the search for neutrinos to inclined directions with respect to the vertical to ground, in particular with zenith angles between $\sim 60°$ and $\sim 95°$. Thus, at each instant, neutrinos can be efficiently detected only from a specific portion of the sky corresponding to these zenith angle ranges. A point-like source of declination δ and right ascension α (equatorial coordinates) is seen at the Auger latitude ($\lambda = -35.2°$), at a given local sidereal time t, with a time-dependent zenith angle $\theta(t)$ as the Earth rotates given by:

$$\cos\theta(t) = \sin\lambda \sin\delta + \cos\lambda \cos\delta \sin(2\pi t/T - \alpha) \ , \quad (1)$$

where T is the duration of one sidereal day. From equation 1, it can be easily obtained that the SD of the Pierre Auger Observatory is sensitive to point-like sources of neutrinos over a broad declination range between $\delta \sim -85°$ to $\delta \sim 60°$ [35, 36]. The exposure of the SD as a function of the neutrino energy and of the source position in the sky, $\mathcal{E}(E_\nu, \delta)$, is evaluated by folding the SD area with the neutrino interaction probability and the selection efficiency for each neutrino channel. The procedure is identical to that used for the calculation of the exposure for a diffuse flux of UHEν outlined before with the exception of the solid angle integration over the sky [35]. The exposure was obtained for the whole data taking period up to 30 June 2018. Only those periods of time when the source is in the field of view of Auger in inclined directions contribute to the exposure.

Given the declination-dependent exposure $\mathcal{E}(E_\nu, \delta)$ upper bounds on the normalization $k_{90}^{\rm PS}(\delta)$ of a differential E_ν^{-2} neutrino flux can also be obtained as a function of declination. These are shown in Fig. 4. The calculation implicitely assumes that the source is emitting continously during the whole period of data taking. The shape of the declination-dependent upper limits is largely determined by the fraction of time a source is within the field of view of the ES or DG analyses. The sensitivity peaks at declinations around $\delta = -53°$ and $+55°$ mostly driven by the fraction of time (around four hours per day) those directions in the sky fall in the field of view of Auger in the highly sensitive angular range (90°, 95°) where Earth-Skimming tau neutrinos dominate the expected rate of events. Auger has an unmatched sensitivity to sources of UHE neutrinos in the Northern terrestrial hemisphere, a region in the sky with no access for experiments such as IceCube due to the opacity of the Earth to EeV neutrinos in those directions when seen from the South Pole.

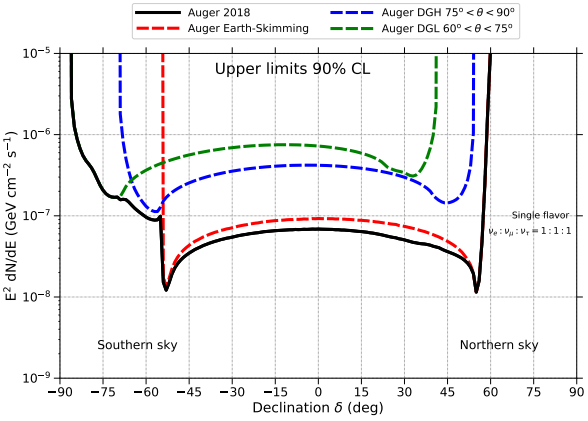

Figure 4. Pierre Auger Observatory upper limits at 90% C.L. on the normalization $k^{\rm PS}$ of a single flavour point-like flux of UHE neutrinos $dN/dE_\nu = k^{\rm PS} E_\nu^{-2}$ as a function of the source declination δ. A $\nu_e : \nu_\mu : \nu_\tau = 1 : 1 : 1$ flavor ratio at Earth is assumed. Auger data up to 30 June 2018.

The detection of the first gravitational wave events GW1501914 [16] and GW151226 [17] from the merging of binary black hole (BBH) systems at cosmological distances marked the birth of GW astronomy. Up to now 10 BBH systems have been identified and the first catalog of GW sources has been recently released by LIGO and Virgo [19]. Even though BBH systems are not expected to emit electromagnetic radiation or neutrinos unless there is matter debris and magnetic fields possibly remaining from the BH progenitors [37, 38], a search for UHE neutrinos was performed with Auger from the first two detected GW events [39]. The search was performed ±500 s around the UTC times at which the BBH systems were observed in GW and one day after their occurrence [39]. The chosen intervals are motivated by the possible association of the merging of compact objects to Gamma Ray Bursts (GRB) [40], an association that has been confirmed in the case of the short GRB 170817A [41]. Neutrinos in a large range of energies have been postulated to be produced in the prompt phase and afterglow phases of the GRB in interactions of accelerated cosmic rays with photons of the GRB. The 1000 s time window represents an upper bound to the

duration of the prompt GRB phase [42], while the one-day window corresponds to a conservative bound of the duration of the afterglow [40].

After applying the same neutrino selection criteria as described above, no neutrino candidates were identified in Auger data in coincidence with any of these GW events in any of the time windows. Assuming a differential neutrino flux E_ν^{-2}, upper bounds on the energy radiated in the form of neutrinos in the energy band (10^{17} eV, 2.5×10^{19} eV) from these events were obtained. The bound for the case of GW151226 and for the one-day search period is shown in Fig. 5 as a function of declination since these events were poorly localized in the sky. The most restrictive bound for GW151226 is obtained for $\delta = +55°$ and would correspond to a total energy radiated in UHE neutrinos smaller than $\sim$ 44% of the energy radiatied by GW151226 in the form of GW ($\sim$ 1 solar masses). A similar bound is obtained for GW150914 because the distances to both mergers are similar and the sensitivity of the SD of Auger is rather stable in time. For GW150914 this fraction is roughly a factor of 3 smaller because the radiated energy in GW is $\sim$ 3 times larger in this case. The constraints obtained are compatible with expectations of absence of neutrino production in naked BBH mergers.

Future detection of BBH mergers closer to us and with better localization could provide more stringent constraints on neutrino production especially if the source happens to be localized in the field of view of the ES and DG neutrino analyses. This was in fact the case for the Binary Neutron Star (BNS) merger GW170817 observed by the LIGO detectors in 2017 [41]. In this case electromagnetic radiation was produced in the form of a GRB only $\sim$ 2 s after the merger and a kilonova was generated that emitted radiation in a broad range of wavelengths from radio to X-rays. The observation at optical frequencies allowed its precise localization in the outskirts of the galaxy NGC 4993 at a distance of $\sim$ 40 Mpc and equatorial coordinates $\alpha(J2000.0) = 13^{\rm h}09^{\rm m}48^{\rm s}$, $\delta(J2000.0) = -23°22'53.''343$ [44]. The source of GW170817 was located just below the horizon as seen from the Auger site, in the field of view of the most sensitive neutrino analysis, namely that searching for ES tau neutrinos. UHE neutrinos were searched for in a time window ±500 s about the detection time of GW170817 while the source was transiting in zenith angle as seen at Auger from $\theta \sim 93.3°$ to $\theta \sim 90.4°$ as shown in Fig. 6. No neutrino candidates were identified and this resulted in the best upper bound to neutrino emission from a BNS system in the 10^{17} to 2.5×10^{19} eV energy interval, complementary to those obtained with IceCube and ANTARES neutrino detectors at lower energies (see Fig.2 in [43]). The search was also made in a longer time window of 14 days to test predictions from longer-lasting emission processes in these type of systems. In this case the Auger limits at EeV energies are comparatively weaker than those from IceCube and ANTARES because the BNS is only observed less than one hour per day in the Earth-Skimming directions where the search for neutrinos is most efficient and a few hours in the Downward-going ones (see Fig. 6 and Fig. 2 in [43]). Neutrino bounds obtained with the Pierre Auger Observatory, IceCube and ANTARES are consistent with predictions from a GRB viewed at a large off-axis angle relative to the jet axis (assumed to be parallel to the rotation axis) where neutrino production is expected to be more copious [40].

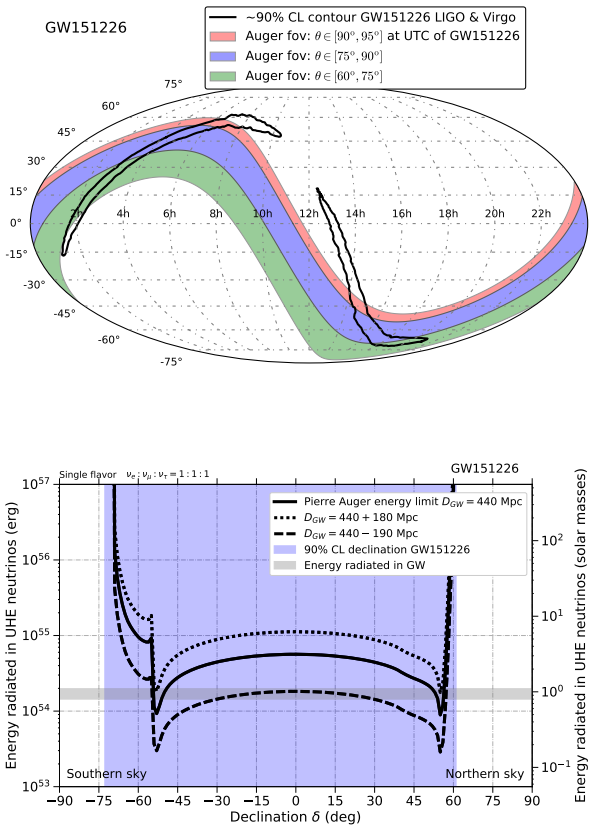

Figure 5. Top: Sky map of the field of view of the Pierre Auger Observatory in equatorial coordinates at the instant of detection of the binary black hole merger event GW151226 by Advanced LIGO. The band limits from top to bottom correspond to lines of zenith angles 95°, 90°, 75° and 60°. The black contours give the 90% C.L. region of the localization of the BBH merger. Bottom: Upper limit at 90% C.L. to the total energy in UHE neutrinos in the 10^{17} to 2.5×10^{19} eV range as a function of declination. The blue shaded band is the 90% C.L. of the reconstructed source declination, and the gray band the energy radiated in the form of GW accounting for uncertainties in distance to the source [17].

One month later than GW170817 on September 17 the IceCube neutrino observatory discovered a $\sim$ 270 TeV muon neutrino pointing to a powerful blazar TXS 0506+056 that was in a gamma-ray flaring state at equatorial declination $\delta \simeq 5.7°$ [20]. When looking in archival data, an excess of 13 ± 5 neutrino events over atmospheric neutrino background from the same direction was also identified in a 110-day time window [21]. These observations constitute $\sim 3.5\sigma$ evidence for the first identified source of high-energy neutrinos. Since TXS 0506+056 is in the field-of-view of the Auger Observatory in the ES (DG) directions for $\sim$ 0.8 ($\sim$ 5.1) hours per day a coincident search for UHE neutrinos was performed with no candidates identified. The details of this search and the bounds obtained are to be reported elsewhere [45].

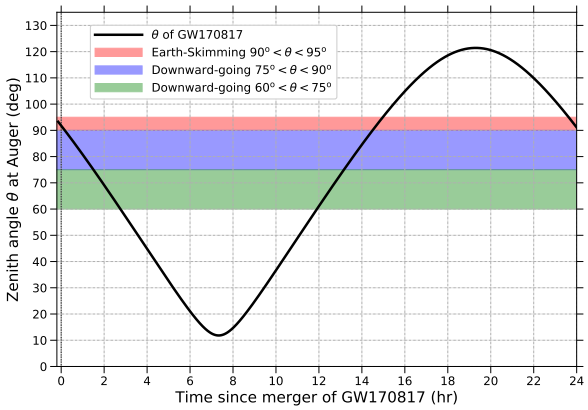

Figure 6. Zenith angle θ of the direction of the source of GW1701817 as viewed from the center of the Surface Detector of the Pierre Auger Observatory in a period of one day. The band limits from top to bottom correspond to lines of zenith angles $\theta = 95°, 90°, 75°$ and $60°$. The source of GW170817 transits along the sky from $\theta \sim 11.8°$ to $\theta \sim 121.4°$ in one day. It is in the field of view of the Earth-Skimming tau neutrino analysis during several periods in one sidereal day, in particular at the moment of emission of GW170817 (coincident with the origin of time in this figure).

3 Photons in Auger

The search for UHE photon primaries in Auger is based on the different development and particle content of photon and hadron-induced air-showers. Combining measurements from both the SD and the FD detectors collected in the so-called hybrid events yields a wealth of information on shower development in the atmosphere that allows the efficient separation of photons and charged cosmic rays.

The main observable for the search for photons with hybrid data is the depth of shower maximum $X_{\rm max}$ that is directly measured with the FD. At a fixed energy photon-induced showers develop on average deeper in the atmosphere than hadronic showers and have larger $X_{\rm max}$. Other observables related to the lateral shower profile on the ground that is measured with the SD are used to complement the information on shower development. In general, photon-induced air showers have a steeper lateral profile and consequently a smaller footprint on the ground and thus a smaller number of triggered SD stations ($N_{\rm stat}$) compared to those initiated by hadrons. To exploit the differences in the lateral development between the different primary particle types an observable S_b was constructed from the signals S_i of each of the triggered stations in the events and their distances r_i to the shower axis as measured on the ground:

$$S_b = \sum_i^{N_{\rm stat}} S_i \left(\frac{r_i}{r_0}\right)^b \qquad (2)$$

where $r_0 = 1000$ m is a reference distance and b a constant [46].

The three observables $X_{\rm max}$, $N_{\rm stat}$ and S_b have been combined in a multivariate analysis (boosted decision tree, BDT) to maximize the photon/hadron discrimination power. For this purpose photon-induced simulated showers with energy above 10^{17} eV and zenith angles between 0° and 65° have been compared to background hadron-induced showers. The BDT distribution is shown in Fig. 7 for the data and the simulated photon and proton samples. To identify photons, a candidate cut is defined at the median of the BDT response distribution for primary photons corresponding by definition to a photon selection efficiency of 50%. The background contamination is 0.14% under the worst-case assumption of a pure proton composition. An important remark is that the discrepancy between data and proton simulations seen in Fig. 7 is consistent with current experimental indications of a change to a heavier composition in the EeV range [5, 48] and the muon deficit observed in simulations with respect to Auger data [47, 49].

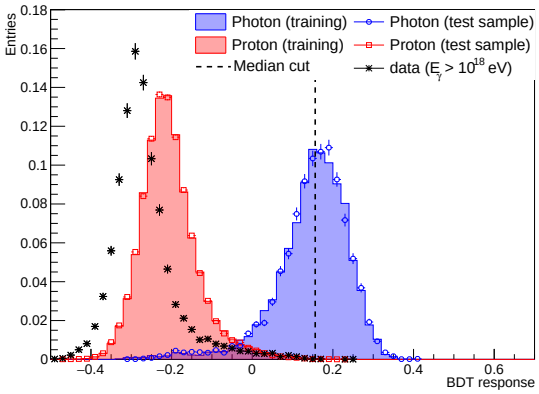

Figure 7. Distribution of the Boosted-Decision-Tree response for the data sample (asterisks), photon simulations (blue-shaded histogram and circles), and proton background sample (red-shaded histogram and squares). The photon candidate cut at the median of the photon distribution is indicated by the dashed line.

The analysis was applied to Auger hybrid data collected between January 2005 and December 2013. Three events passed the photon cut as can be seen in Fig. 7, the number of photon-like events being compatible with the proton background expectation of 11.4 events. Upper limits on the integral photon flux at 95% C.L. are derived in [9] assuming zero background events, a power-law spectrum E^{-2} and using the integrated exposure from MC simulations [9]. For energy thresholds of 1, 2, 3, 5 and 10 EeV the fraction of photons in the all-particle flux is smaller than 0.1%, 0.15%, 0.33%, 0.85% and 2.7% respectively. The three candidate events all have energies close to 1 EeV, so the observed number is zero for all but the first energy threshold. The upper limits are shown in Fig. 8 and impose tight constraints on top-down scenarios proposed to explain the origin of UHE cosmic rays (see [9] for a full list of references). We are also starting to constrain the most optimistic models of UHE photon production in interactions of a pure UHE proton flux with the CMB, in line with the constraints obtained from the non-observation of UHE neutrinos in Auger presented in the previous section.

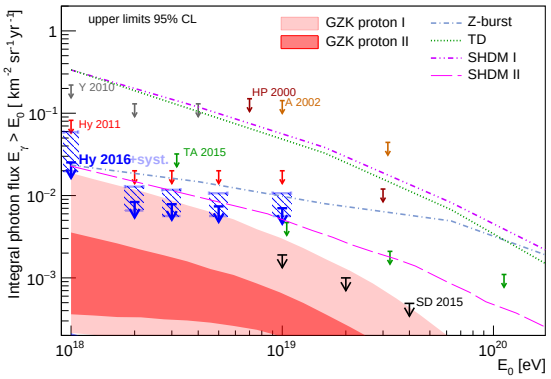

Figure 8. Upper limits on the integral photon flux (blue arrows, Hy 2016) with hybrid data collected between January 2005 and December 2013[9]. When the systematic uncertainties of the detector are taken into account the obtained limits are indicated by the light-blue dashed boxes around the blue arrows. Also shown are the limits previously published by the Pierre Auger Observatory (Hy 2011 and SD 2015) and other experiments (Telescope Array, Yakutsk, AGASA, Haverah Park). The shaded regions and the lines give the predictions for photon fluxes from cosmogenic models and several top-down models (Z-burst, topological defects, super-heavy dark matter, see [9] for a full list of references.

The good angular resolution of the hybrid analysis (typically $< 1°$) also allows to search for UHE photons from point-like sources in the sky. A photon point source would be detectable through an excess of photon-like events from a certain direction. The analysis uses hybrid events from the same period as in the search for a diffuse flux of photons (January 2005 to December 2013), but in the energy range ($10^{17.3}$ to $10^{18.5}$ eV) to take advantage of the higher statistics at lower energies. A targeted search for UHE photons was performed restricting the analysis to predefined classes of sources to reduce the statistical penalty of many trials and complement previous blind searches [50]. Since the attenuation length of photons in the energy range considered varies between ~ 0.1 and ~ 1 Mpc, the target sources contain only Galactic objects (millisecond pulsars, γ-ray pulsars, low- and high-mass X-ray binaries and the Galactic center), as well as some nearby extragalactic ones, namely three powerful γ-ray emitters in the Large Magellanic Cloud and the core region of Centaurus A. A more detailed description can be found in [10]. Photon-like events are selected using a BDT trained with MC simulations of photon- and proton-induced air shower events with $X_{\rm max}$ and S_b as main variables complemented by additional observables (see [10] for full details). Photon candidates are selected through a cut in the BDT response optimized for each target direction. Averaged over all target directions, the photon selection retains 81.4% of simulated primary photons with a background rejection of 95.2%. A p-value is assigned to each candidate source, taking into account the observed number of events from that direction as well as the expected number of background events. The p-values of all targets in a class of sources are combined with and without weights proportional to both the directional exposure for photons and the measured electromagnetic flux from the source (taken from astrophysical catalogs). All combined or individual p-values have a statistical significance smaller then 3σ. This result allows us to conclude that there is no evidence in Auger data for photon emission neither from any of target classes considered nor from individual sources.

4 Conclusions

The Pierre Auger Observatory is a key detector in the field of Multi-messenger Astrophysics at EeV energies. With Auger, we can discriminate photons and neutrinos in the much larger background of charged CR at EeV energies, with large identification efficiency.

No neutrinos or photons were unambiguously identified in the EeV energy range, and upper bounds to their diffuse flux were obtained that constrain neutrino and photon production in interactions of a pure proton flux with the CMB for sources that evolve strongly with redshift.

With the SD of Auger, we can also search for neutrinos from point-like sources, monitoring a large fraction of the sky (from $\sim -85°$ to $\sim 60°$) in equatorial declination with peak sensitivities at declinations around $-53°$ and $+55°$ and unmatched ones in the Northern hemisphere. An unrivaled sensitivity can also be obtained in the case of transient sources of order an hour or less if they occur when the source is in the field of view of the ES and DG channel [51] with the BNS merger detected by Advanced LIGO as a paradigmatic example. No neutrinos were detected neither from BBH mergers observed in GW nor in spatial coincidence with the blazar TXS 0506+056.

The search for point-like sources of UHE photons yielded no significant deviations from background expectations for Galactic sources and nearby extragalactic sources, the only targets accessible with photons in the EeV range.

The Pierre Auger Observatory is also a follow-up and triggering observatory in the Astrophysical Multimessenger Observatory Network (AMON) [52]. In particular Auger sends all vertical $\theta \geq 60°$ events with energy ≥ 3 EeV to AMON with the goal of performing real-time coincidence analysis with other observatories IceCube, HAWC, etc... Two or more events observed within 100 s and $< 3°$ generate an AMON alert for other AMON-partner observatories to follow-up on.

Presently, the Observatory is being upgraded to AugerPrime to primarily improve the mass composition measurements and particle physics capabilities with the surface detector array (see [53, 54] for details). Also each WCD station will be enhanced by including a radio antenna to provide improved information of air showers [55]. These new features and capabilities will open up many new possibilities for improved searches of photons and neutrinos to strengthen the role of the Pierre Auger Observatory as a multi-messenger observatory at EeV energies.

References

[1] A. Aab *et al.* [Pierre Auger Collaboration], Nucl. Instrum. Meth. A **798**, 172 (2015).
[2] A. Aab *et al.* [Pierre Auger Collaboration], to appear in Frontiers in Physics (2019).
[3] V. Verzi for the Pierre Auger Collaboration, these proceedings.
[4] P. L. Ghia for the Pierre Auger Collaboration, these proceedings.
[5] M. Unger for the Pierre Auger Collaboration, these proceedings.
[6] M. Roth *et al.* for the Pierre Auger Collaboration, these proceedings.
[7] A. Aab *et al.* [Pierre Auger Collaboration], arXiv:1708.06592 [astro-ph.HE]
[8] C. Bleve for the Pierre Auger Collab., PoS (ICRC2015) 1103.
[9] A. Aab *et al.* [Pierre Auger Collab.], JCAP **04**, 009 (2017).
[10] A. Aab *et al.* [Pierre Auger Collab.], Astrophys. J. **837**, L25 (2017).
[11] A. Aab *et al.* [Pierre Auger Collab.], Phys. Rev. D **91**, 092008 (2015)
[12] L. A. Anchordoqui et al., Journal of High Energy Astrophysics, **1**, 1 (2014).
[13] B. Baret and V. Van Elewyck, Rep. Prog. Phys. **74**, 046902 (2011).
[14] D. Seckel and T. Stanev, Phys. Rev. Lett. **95**, 141101 (2005).
[15] A. De Angelis, G. Galanti, M. Roncadelli, Mon. Not. Roy. Astron. Soc. **432**, 3245 (2013).
[16] B. P. Abbott *et al.* [LIGO Scientific Collaboration, Virgo Collaboration], Phys. Rev. Lett. **116**, 061102 (2016);
[17] B. P. Abbott *et al.* [LIGO Scientific Collaboration, Virgo Collaboration], Phys. Rev. Lett. **116**, 241103 (2016);
[18] B. P. Abbott *et al.* [LIGO Scientific Collaboration, Virgo Collaboration], Phys. Rev. Lett. **118**, 221101 (2017).
[19] B. P. Abbott *et al.* [LIGO Scientific Collaboration, Virgo Collaboration], arXiv:1811.12907 [astro-ph.HE].
[20] M. G. Aartsen *et al.* [IceCube Collab.], Science **361**, 146 (2018)
[21] M. G. Aartsen *et al.* [IceCube Collab.], Science **361**, 147 (2018)
[22] J. Abraham *et al.* [Pierre Auger Collab.], Nucl. Instrum. Meth. A **620**, 227 (2010).
[23] D. Fargion, Astrophys. J. **570**, 909 (2002); A. Letessier-Selvon, AIP Conf. Proc. **566**, 157 (2001).
[24] J. Abraham *et al.* [Pierre Auger Collab.], Phys. Rev. D **84**, 122005 (2011).
[25] J. Abraham *et al.* [Pierre Auger Collab.], Phys. Rev. D **79**, 102001 (2009).
[26] G. J. Feldman and R. D. Cousins, Phys. Rev. D **57**, 3873 (1998).
[27] M. G. Aartsen *et al.* [IceCube Collab.], Phys. Rev. D **98**, 062003 (2018).
[28] M. Ahlers *et al.*, Astropart. Phys. **34**, 106 (2010).
[29] K. Kotera, D. Allard, and A. Olinto, JCAP **10**, 013 (2010).
[30] R. Aloisio, D. Boncioli, A. di Matteo, A. F. Grillo, S. Petrera, and F. Salamida, JCAP **10**, 006 (2015).
[31] K.-H. Kampert, M. Unger, Astropart. Phys. **35**, 660 (2012).
[32] E. Waxman and J. Bahcall, Phys. Rev. D **59**, 023002 (1999); E. Waxman in Neutrino Astronomy: Current Status, Future Prospects Edited ny: T.K. Gaisser and A. Karle. arXiv:1511.00815v1 [astro-ph.HE].
[33] A. Aab *et al.* [Pierre Auger Collab.], JCAP **08**, 019 (2014).
[34] P. W. Gorham *et al.* [ANITA Collaboration], Phys. Rev. D **98**, 022001 (2018).
[35] P. Abreu *et al.* [Pierre Auger Collab.] Astrophys. J. Lett. **755**, L4 (2012).
[36] E. Zas for the Pierre Auger Collaboration, PoS (ICRC2017) 972.
[37] K. Murase *et al.*, Astrophys. J. Lett. **822**, L9 (2016) L9
[38] K. Kotera and J. Silk, Astrophys. J. Lett. **823**, L29 (2016).
[39] A. Aab *et al.* [Pierre Auger Collab.], Phys. Rev. D **94**, 122007 (2016).
[40] P. Mészáros, Rept. Prog. Phys. **69**, 2259 (2006).
[41] B. P. Abbott *et al.* [LIGO Scientific Collaboration, Virgo Collaboration], Astrophys. J. Lett. **848**, L12 (2017).
[42] B. Baret *et al.*, Astropart. Phys. **35**, 1 (2011).
[43] A. Albert *et al.* [ANTARES, IceCube, Pierre Auger and LIGO/Virgo Collabs.], Astrophys. J. Lett. **850**, L35 (2017).
[44] D. A. Coulter *et al.* Science **358**, 1556 (2017).
[45] A. Aab *et al.* [Pierre Auger Collab.], in preparation (2019).
[46] G. Ros *et al.*, Astropart. Phys. **47**, 10 (2013).
[47] A. Aab *et al.* [Pierre Auger Collab.], Phys. Rev. D **91**, 032003 (2015); Erratum: Phys. Rev.D **91**, 059901 (2015).
[48] J. Bellido for the Pierre Auger Collaboration, PoS (ICRC2017) 506.
[49] A. Aab *et al.* [Pierre Auger Collab.], Phys. Rev. Lett. **117**, 192001 (2016)
[50] A. Aab *et al.* [Pierre Auger Collab.] Astrophys. J. **789**, 160 (2014).
[51] A. Aab *et al.* [Pierre Auger Collab.], in preparation (2019).
[52] M. W. E. Smith *et al.*, Astropart. Phys. **45**, 56 (2013).
[53] D. Martello for the Pierre Auger Collaboration, PoS (ICRC2017) 383.
[54] A. Castellina for the Pierre Auger Collaboration, these proceedings.
[55] J. Hörandel for the Pierre Auger Collaboration, these proceedings.